Heat Transfer and Pressure Drop During Condensation of Refrigerant 134a in an Axially Grooved Tube

D. M. Graham, J. C. Chato, and T. A. Newell

ACRC TR-114 March 1997

For additional information:

Air Conditioning and Refrigeration Center
University of Illinois
Mechanical & Industrial Engineering Dept.
1206 West Green Street
Urbana, IL 61801

(217) 333-3115

Prepared as part of ACRC Project 74
Experimental Investigation of Void Fraction
During Refrigerant Condensation and Evaporation
J. C. Chato and T. A. Newell, Principal Investigators

The Air Conditioning and Refrigeration Center was founded in 1988 with a grant from the estate of Richard W. Kritzer, the founder of Peerless of America Inc. A State of Illinois Technology Challenge Grant helped build the laboratory facilities. The ACRC receives continuing support from the Richard W. Kritzer Endowment and the National Science Foundation. The following organizations have also become sponsors of the Center.

Amana Refrigeration, Inc.
Brazeway, Inc.
Carrier Corporation
Caterpillar, Inc.
Copeland Corporation
Dayton Thermal Products
Delphi Harrison Thermal Systems
Eaton Corporation
Ford Motor Company
Frigidaire Company
General Electric Company
Hydro Aluminum Adrian, Inc.
Indiana Tube Corporation
Lennox International, Inc.
Modine Manufacturing Co.
Peerless of America, Inc.
Redwood Microsystems, Inc.
The Trane Company
Whirlpool Corporation
York International, Inc.

For additional information:

Air Conditioning & Refrigeration Center
Mechanical & Industrial Engineering Dept.
University of Illinois
1206 West Green Street
Urbana IL 61801

217 333 3115

Heat Transfer and Pressure Drop During Condensation of Refrigerant 134a in an Axially Grooved Tube

Doug M. Graham, John C. Chato and Ty A. Newell[1]

ABSTRACT

R134a condensation experiments have been performed over a mass flux range of 75 to 450 kg/m^2-s (55 to 330 klb$_m$/ft^2-hr) in an 8.91 mm (0.351") inside diameter, axially grooved, micro-fin tube. At 75 kg/m^2-s (55 klb$_m$/ft^2-hr), the axially grooved tube performs marginally better than a smooth tube, but worse than a similarly grooved tube with an 18 degree helix angle over a broad range of refrigerant qualities. Mass fluxes at 150 kg/m^2-s (110 klb$_m$/ft^2-hr) and greater show broad quality ranges in which the axially grooved tube performs significantly better than both smooth and helically grooved tubes. Examination of a Froude rate parameter indicates that the axially grooved tube is able to maintain an annular film flow characteristic that results in more efficient heat transfer. Pressure drop characteristics of the axially grooved tube are similar to those found in an 18 degree helix angle tube.

NOMENCLATURE

c_p	specific heat at constant pressure	
$c_{p,l}$	specific heat at constant pressure for liquid refrigerant	
D	diameter	
$D_{eq,flow}$	equivalent flow diameter	
EF	enhancement factor	
Fr_l	liquid-only Froude number	$(G/\rho_l)^2/gD$
Fr_{so}	Soliman's modified Froude number	equations (8), (9)
Ft	Froude rate parameter	equations (18), (19)
G	mass flux	
g	gravitational acceleration	
Ga	Galileo number	$\rho_l(\rho_l-\rho_v)D^3/\mu_l^2$
i_{lv}	enthalpy of vaporization	
Ja	Jakob number	$c_p(T_{sat}-T_s)/i_{lv}$
k	thermal conductivity	
k_l	liquid thermal conductivity	
$\dot{m}$	mass flow rate	
m_l	liquid mass flow rate	
m_v	vapor mass flow rate	
Nu	Nusselt number	
PF	penalty factor	

[1] author to whom comments should be addressed; (217-333-1655; t-newell@uiuc.edu)

Pr	Prandtl number	$\mu c_p/k$
Pr_l	liquid Prandtl number	$\mu c_{p,l}/k_l$
Re_l	liquid Reynolds number	$GD(1-x)/\mu_l$
Re_{vo}	vapor only Reynolds number	GD/μ_v
V_v	vapor velocity	
x	quality	
x_i	inlet quality	
x_o	outlet quality	
X_{tt}	Lockhart Martinelli number	equation (6)
α	void fraction	
α_i	inlet void fraction	
α_o	outlet void fraction	
ΔP	pressure drop	
ΔP_{ACC}	acceleration pressure drop	equation (13)
ΔP_{FRIC}	frictional pressure drop	equation (12)
ϕ_l^2	two-phase pressure drop multiplier	
ρ_v	vapor density	
ρ_l	liquid density	
μ	viscosity	
μ_l	liquid viscosity	
μ_v	vapor viscosity	

INTRODUCTION

Enhancement of tube heat transfer without an equivalent increase of pressure drop is an active area of investigation in the refrigeration and air conditioning fields [1-13]. "Micro-fin" enhancements are of special interest because little, if any, additional material is required for inscribing the internal tube surface with structures that can result in high heat transfer increases. Most studies have investigated "helical" micro-fin tubes [3, 5-13] that are more readily available commercially. Additionally, many of the experimental studies have obtained average results rather than local heat transfer and pressure drop data.

Chiang [1] found axial grooved tubes to generally show higher performance than helical tubes over a broad range of mass fluxes and qualities for both evaporation and condensation. Direct comparison between the axial grooved tubes and helical (18 degree) grooved tubes could not be made because the grooves were of significantly different fin geometries and fin frequencies. The 10 mm (.394") diameter tubes had 72 and 60 internal fins for the axial and 18 degree helix grooves, respectively. For the 7.5 mm (.295") diameter tubes, Chiang [1] tested 60 fins for the axial and 43 internal fins for the 18 degree helix groove configuration.

In the present study, a custom fabricated 8.91 mm (.351") diameter tube with 60 axial fins was obtained. The fin geometry and number of fins geometrically matches an 18 degree helix tube made by the manufacturer. The 18 degree helix tube was previously tested at the University of Illinois Air Conditioning and Refrigeration Center's (ACRC) condenser test facility [5, 6]. Investigation of the geometrically similar, axially grooved tube has been undertaken in order to examine trends and performance differences in a detailed manner over a range of refrigerant mass fluxes and qualities. The axial tube, in general, behaves in a significantly different manner than the helical grooved tube.

BACKGROUND

An apparatus has been designed in the ACRC at the University of Illinois that allows in-tube condensation data to be collected over a wide range of operating conditions. In the test-condenser, local, in-tube heat transfer coefficients and pressure drops of the working fluid are measured. A schematic of the apparatus is provided in Fig. 1.

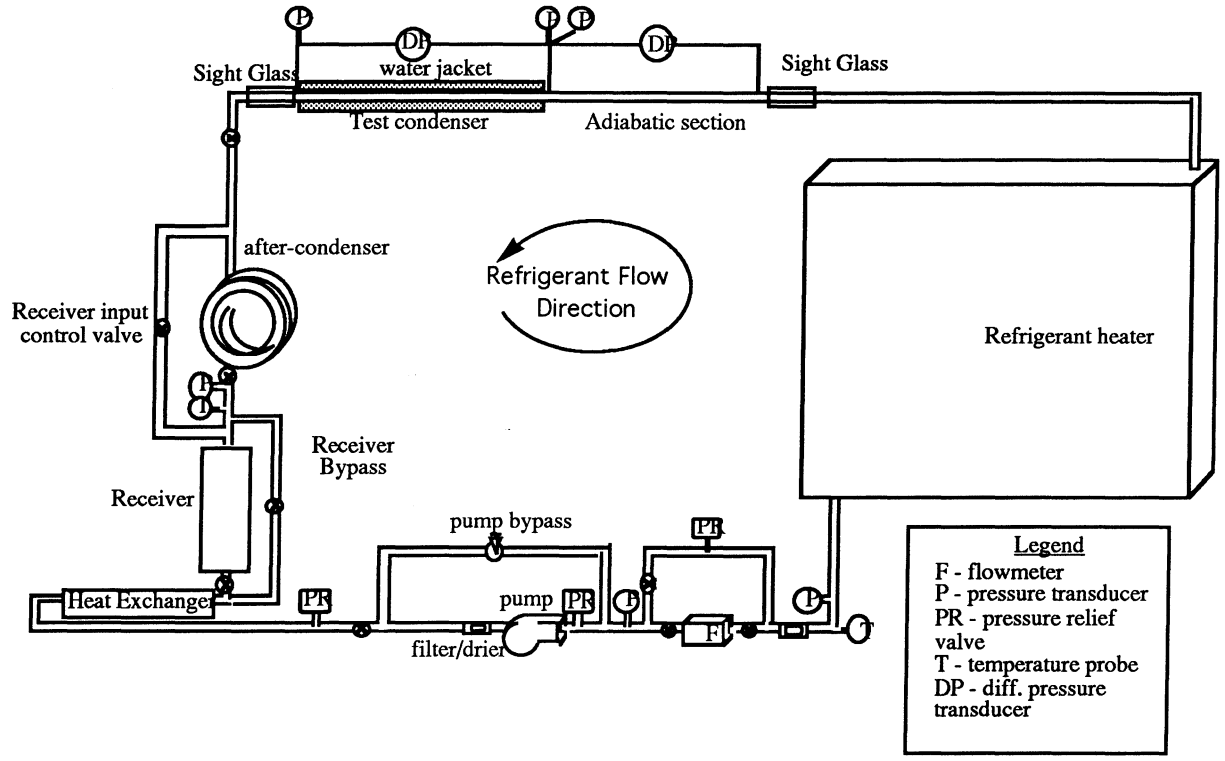

Figure 1 Experimental Apparatus (Dobson [2]).

The refrigerant is circulated through the refrigerant loop by a MicroPump three gear, variable speed pump. This pump needs no lubrication to run, and therefore allows the testing of pure refrigerants, without the addition of oil. The mass flux of the refrigerant is measured immediately

after the pump, either by a Micro-Motion D mass flow meter, or a Max Machinery positive displacement flow meter, depending on the flow rate.

After the pump, the refrigerant is set to the desired condition by the use of a preheater, consisting of a 9.52 mm (0.375") o.d. copper tube. Each pass of the tube is wrapped with resistance heater tapes that are used to input heat to the refrigerant. This allows the experimenter to set the temperature and quality of the refrigerant at the test section inlet. Located systematically throughout the test section are thermocouples which measure the wall temperatures. The thermocouples are staggered in such a way as to measure circumferential and longitudinal temperature distributions at the tube wall. Temperatures were measured with thermocouples that were calibrated with a constant temperature bath, which was found to have an uncertainty of 0.1 °C (0.18 °F).

Located across the test section is a differential pressure transducer, which measures the pressure drop in a length of 1.22 m (48.0"). The uncertainty of this transducer was estimated to be ±1 kPa (±.15 psi). Absolute pressure transducers are also located at the test section inlet, the test section outlet, at the receiver and before the preheater. These transducers were calibrated together on a dead weight tester over their range of applicability. From these tests, the uncertainty of these instruments is estimated at ±7 kPa (±1 psi).

After the refrigerant leaves the test section, it is cooled down to a subcooled liquid by an aftercondenser and water to refrigerant heat exchanger. The refrigerant then passes through a filter and is recirculated through the pump. The temperature of the refrigerant is in part controlled by the heat input from the preheater to the test section, but the majority of the temperature control is obtained by the use of a heated water tank. A refrigerant receiver is placed into this tank, and by varying the temperature of the water in this tank, and the amount of refrigerant that flows through this receiver, the system pressure can be set to the necessary quantity.

Water is used to condense the refrigerant in the test section. The water pressure is maintained at 101.3 kPa (14.7 psi) in order to ensure that there is no air in the water piping. The water flow rate across the test section is set with a rotameter, and the temperature of the water is varied by the use of a water heater. After the heater, the water enters an annulus that is centered around the test section. This annulus is made with a 19.1 mm (0.75") o.d. plastic tube. Inside the tube are a series of plastic mixers that are used to swirl the flow, and maintain a nearly uniform temperature at any longitudinal location. The water flow rate is measured at the discharge with a graduated cylinder and a stopwatch. The entire experimental apparatus including the test section, water section and all the tubing is covered with insulation to minimize losses to the environment, and also to help the system maintain steady state conditions.

The experiments were all run at a saturation temperature of approximately 35 °C (95 °F). Once the desired conditions have been set, and steady state is achieved, data is collected for five minutes.

The test section used in this study is a 9.52 mm (0.375") o.d. tube, which contains sixty trapezoidal fins that are arranged axially inside the tube at an angle of 0° to the axial direction. The maximum inside diameter of the tube is 8.91 mm (0.351") and the minimum inside diameter is 8.53 mm (0.336"). The fins have an average height of 0.180 mm (0.007"). Experiments run by Ponchner [6] are also included in this report. Ponchner's experiments were run on the same apparatus and his test section differed from the current test section only by the fact that its sixty trapezoidal fins were arranged helically inside the tube at an angle of 18°. Fig. 2 shows the cross section of the microfinned tube used in this study and the one used by Ponchner [6].

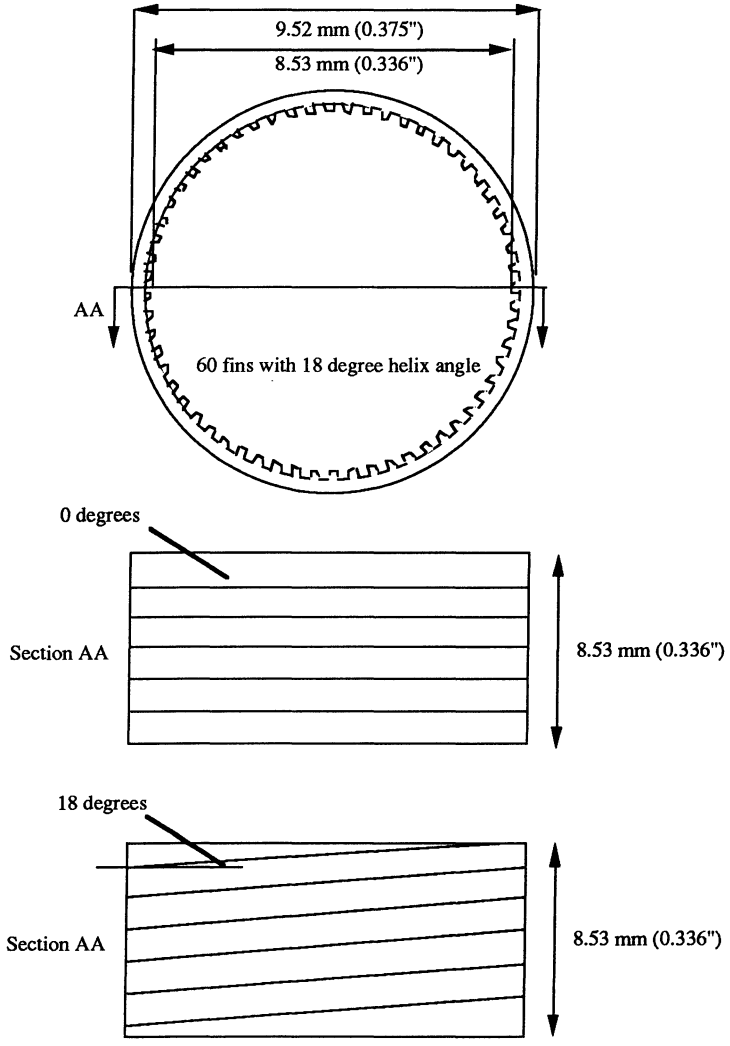

Figure 2 Cross section of the microfinned test sections.

In this study two parameters are used to compare the performance of the microfinned tubes to the performance of a similar smooth tube. The first parameter compares the heat transfer characteristics, while the second compares the pressure drop characteristics.

The parameter used to compare the heat transfer characteristics is the enhancement factor, EF. For the purpose of this study, the enhancement factor is defined to be the ratio of the heat transfer of the enhanced tube to the heat transfer of a similar smooth tube, operating at the same conditions.

$$EF = \left(\frac{\dot{Q}_{microfin}}{\dot{Q}_{smooth}} \right)_{same\ conditions}$$

Here the heat transfer rate for the two tube geometries can be defined with the following equations:

$$\dot{Q}_{microfin} = h_{microfin} A_{microfin} \Delta T$$

$$\dot{Q}_{smooth} = h_{smooth} A_{smooth} \Delta T$$

Since ΔT is the same in both equations, the enhancement factor can be represented as the heat transfer enhancement multiplied by the area ratio. If the area of the smooth tube is taken as the area of a smooth tube with an inside diameter equal to the maximum inside diameter of the microfinned tubes, the area ratio becomes 1.62.

$$EF = \left(\frac{h_{microfin}}{h_{smooth}} \right) A_{rat} = 1.62 \left(\frac{h_{microfin}}{h_{smooth}} \right) \tag{1}$$

The heat transfer coefficient for the comparable smooth tube was calculated using a Dobson correlation [2], which is divided into a wavy flow correlation and an annular flow correlation. The form of the annular correlation is the following:

$$Nu = 0.023 Re_l^{0.8} Pr_l^{0.4} \left[1 + \frac{2.22}{X_{tt}^{0.889}} \right] \tag{2}$$

The wavy correlation is the following:

$$Nu = \frac{0.23 Re_{vo}^{0.12}}{1 + 1.11 X_{tt}^{0.58}} \left[\frac{Ga\,Pr}{Ja} \right]^{0.25} + (1 - \theta_l / \pi) Nu_{forced} \tag{3}$$

where:

θ_l = angle subtended from the top of the tube to the liquid level

$$Nu_{forced} = 0.0195 Re_l^{0.8} Pr_l^{0.4} \phi_l(X_{tt}) \tag{4}$$

where:

$$\phi_l(X_{tt}) = \sqrt{1.376 + \frac{c_1}{X_{tt}^{c_2}}} \tag{5}$$

The turbulent-turbulent Lockhart-Martinelli parameter [14] can be calculated by:

$$X_{tt} = \left(\frac{\rho_v}{\rho_l}\right)^{0.5}\left(\frac{\mu_l}{\mu_v}\right)^{0.1}\left(\frac{1-x}{x}\right)^{0.9} \tag{6}$$

For $0<Fr_l\leq 0.7$:

$c_1=4.172+5.48Fr_l-1.564Fr_l^2$

$c_2=1.773-0.169Fr_l$

For $Fr_l>0.7$:

$c_1=7.242$

$c_2=1.655$

The liquid level angle, θ_l, can be related to the void fraction by the following equation, if the area occupied by the condensate film is neglected:

$$\alpha = \frac{\theta_l}{\pi} - \frac{\sin(2\theta_l)}{2\pi} \tag{7}$$

Dobson [2] also recommended the conditions under which each of the correlations should be used. The parameter used to predict the flow regime is the Froude number, as defined by Soliman[15]. For a $Fr_{so}<20$, Dobson [2] recommends that the wavy correlation be used, and for $Fr_{so}>20$ Dobson [2] recommends that the annular form of the correlation be used.

where:

$$Fr_{so} = 0.025Re_l^{1.59}\left(\frac{1+1.09X_{tt}^{0.039}}{X_{tt}}\right)^{1.5}\frac{1}{Ga^{0.5}} \text{ for } Re_l \leq 1250 \tag{8}$$

$$Fr_{so} = 1.26Re_l^{1.04}\left(\frac{1+1.09X_{tt}^{0.039}}{X_{tt}}\right)^{1.5}\frac{1}{Ga^{0.5}} \text{ for } Re_l > 1250 \tag{9}$$

Along with the heat transfer enhancement of the microfinned tube, there is also a penalty factor due to the increased pressure drop generated by the fins. Here the penalty factor, PF, is

defined as the ratio of the pressure drop found in the microfinned tube to the pressure drop of a similar smooth tube operating at the same conditions, over the same length.

$$PF = \left(\frac{\Delta P_{microfin}}{\Delta P_{smooth}} \right)_{equal\ length} \tag{10}$$

The corresponding pressure drop for the smooth tube was calculated using the correlation proposed by Souza [16, 17]. This correlation takes into account both frictional and acceleration pressure drops and is defined as:

$$\Delta P_{SMOOTH} = \Delta P_{ACC} + \Delta P_{FRIC} \tag{11}$$

$$\Delta P_{FRIC} = \Delta P_L \phi_L^2 \tag{12}$$

$$\Delta P_{ACC} = \frac{16\dot{m}^2}{\pi^2 D^4} \left\{ \left[\frac{x_o^2}{\rho_V \alpha_o} + \frac{(1-x_o)^2}{\rho_L (1-\alpha_o)} \right] - \left[\frac{x_i^2}{\rho_V \alpha_i} + \frac{(1-x_i)^2}{\rho_L (1-\alpha_i)} \right] \right\} \tag{13}$$

where:

$$\Delta P_L = \frac{2 f_L G^2 (1-x)^2 L}{\rho_L D} \tag{14}$$

$$f_L = \frac{0.079}{Re_L^{0.25}} \tag{15}$$

The void fraction (α) can be calculated using the Zivi [18] correlation:

$$\alpha = \frac{1}{1 + \left(\frac{1-x}{x} \right) \left(\frac{\rho_V}{\rho_L} \right)^{0.67}} \tag{16}$$

It should be noted that the smooth tube diameter used in the above calculations is an equivalent flow diameter, $D_{eq,flow}$. The equivalent flow diameter is related to the cross-sectional inside area of the micro-finned tube by the following equation:

$$A_{cross-sect} = \frac{\pi}{4} (D_{eq,flow})^2 \tag{17}$$

RESULTS

Trends in the axially grooved tube's heat transfer are shown in Fig. 3 over a range of qualities and for mass fluxes from 75 to 450 kg/m^2-s (55 to 330 klb$_m$/ft^2-hr). With the exception of the 75 kg/m^2-s (55 klb$_m$/ft^2-hr) mass flux condition, the axially grooved tube generally outperformed the

18 degree helix angle tube. Plotting the axially grooved tube and the 18 degree helix grooved tube using the enhancement factor defined by equation (1) helps identify important trends in the data.

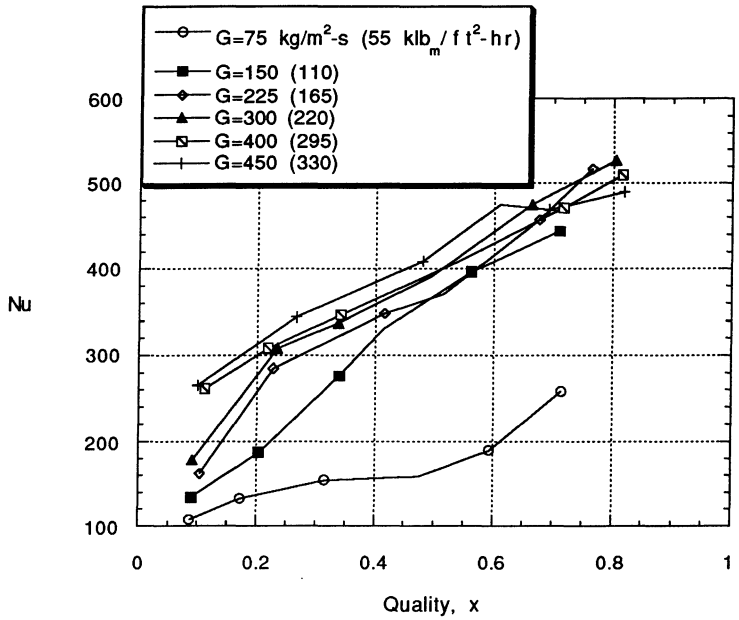

Figure 3 Heat transfer coefficient versus quality for the axially grooved tube over a range of refrigerant mass fluxes.

Figs. 4 to 9 show the axial and 18 degree helix enhancement factors for each mass flux condition. Dobson's [2] correlations for condensation heat transfer have been used for calculating the smooth tube reference heat transfer coefficients. Ponchner's [5] data has been used for the 18 degree helix performance. As previously described, a Froude number of 20 was defined by Dobson as the transition between a stratified wavy dominated flow and an annular liquid film flow. High gas velocities, caused by high quality and/or high mass flux conditions, result in the annular film.

An interesting trend shown in Figs. 4 to 9 is the systematic progression of high levels of enhancement for the axially grooved tube as the mass flux changes. At low mass fluxes the axial tube performs poorly. As the mass flux increases, depending on the quality, increases in heat transfer enhancement significantly above those for the 18 degree helix tube are observed.

At the lowest mass flux tested, as shown in Fig. 4, the enhancement factor for the axially grooved tube is significantly lower than that of the 18 degree helix tube. The 18 degree helix tube shows an enhancement factor somewhat higher than the 62 percent increase in surface area over a smooth tube's internal surface. The axial grooved tube shows an improvement that is only 20 percent greater than the smooth tube. All quality conditions for the low mass flux condition are at Froude numbers less than 20. The enhancement factors, therefore, are based on the tubes' performances relative to the stratified wavy flow heat transfer predictions. The grooves in the axial

tube may be inhibiting fluid from draining into a stratified flow configuration. Additionally, with relatively low vapor velocities, liquid may be locked into the grooves, effectively blocking the vapor from interacting with the tube wall surfaces. The helical tube's enhancement shows that it may somewhat augment the drainage of liquid refrigerant, thus exposing or allowing more of its surface area to participate in heat transfer.

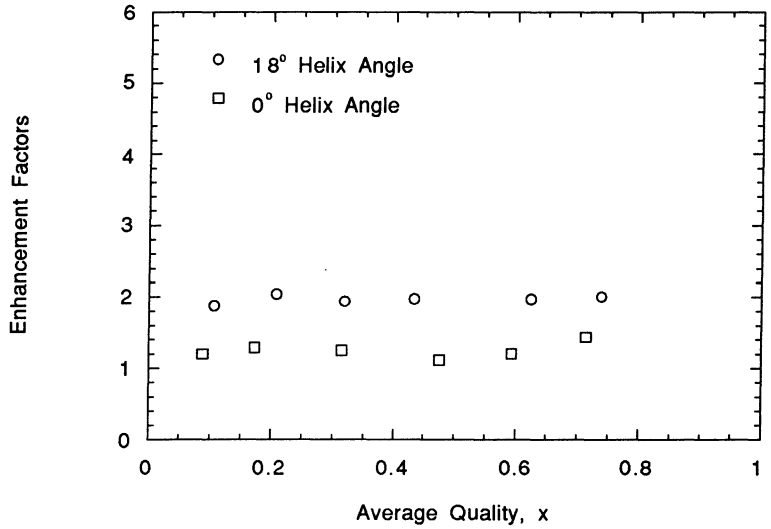

Figure 4 Enhancement factor for the axial and helical tubes over a range of qualities for a mass flux of 75 kg/m^2-s (55 klb$_m$/ft^2-hr).

Increases in mass flux, as shown in Figs. 5 to 9, show regions in which the axial grooved tube's enhancement is significantly higher than the tube's area enhancement effect. At a mass flux of 150 kg/m^2-s (110 klb$_m$/ft^2-hr), as shown in Fig. 5, the enhancement factor is approximately 2.5 at higher qualities. The Froude number for the conditions shown in Fig. 5 are all below 20, requiring that the stratified wavy flow form of Dobson's relation be used for smooth tube heat transfer predictions. The helical tube shows a relatively consistent level of enhancement that is essentially that due to the 62 percent surface area enhancement.

Examining Figs. 6 and 7, reveals that increasing the mass flux to 225 and 300 kg/m^2-s (165 and 220 klb$_m$/ft^2-hr) causes the axial tube's region of significant heat transfer enhancement to move toward lower qualities. The helical tube generally shows a relatively steady enhancement factor that remains near the level expected due to its area enhancement. Peak enhancement factors of 2.5 are obtained for the 225 kg/m^2-s (165 klb$_m$/ft^2-hr) mass flux, while the 300 kg/m^2-s (220 klb$_m$/ft^2-hr) mass flux shows enhancements near 2.6. At high qualities, although the heat transfer coefficients have increased relative to lower quality conditions (see Fig. 3), the level of axial tube

enhancement relative to a smooth tube has diminished. The region where the enhancement level drops, at a quality of approximately 0.6 in Figs. 6 and 7, is where the Froude number is 20, indicating that the flow in a smooth tube would be in an annular flow configuration.

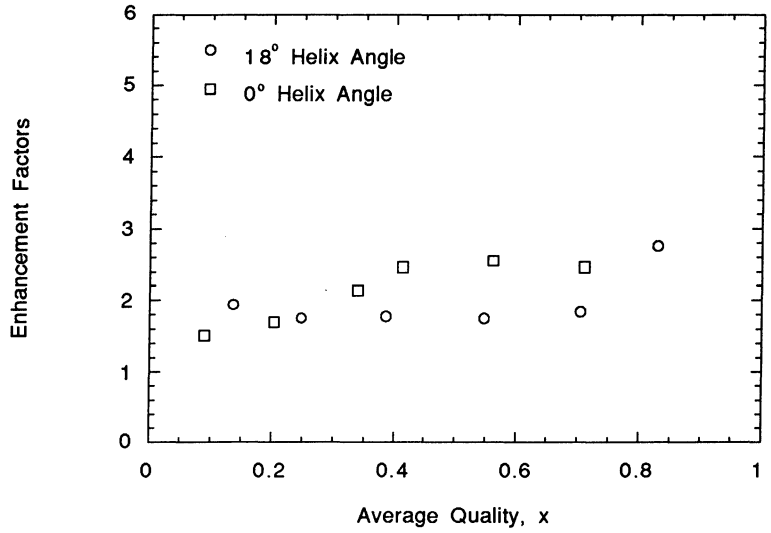

Figure 5 Enhancement factor for the axial and helical tubes over a range of qualities for a mass flux of 150 kg/m^2-s (110 klb$_m$/ft^2-hr).

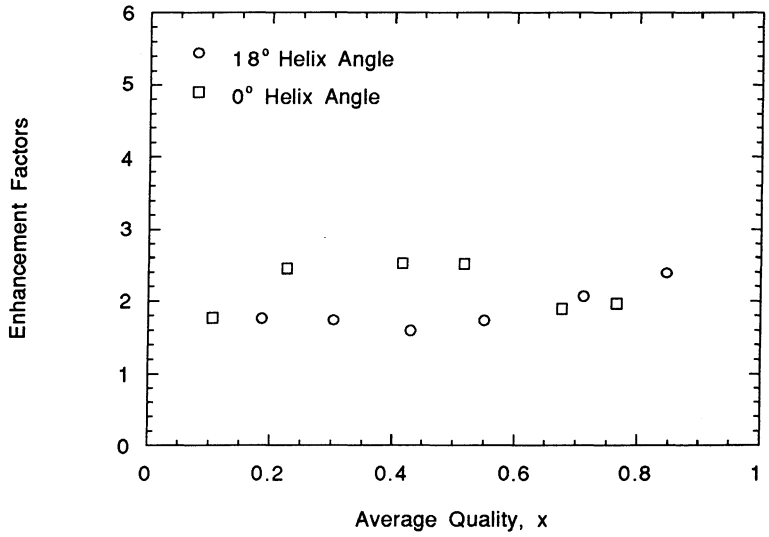

Figure 6 Enhancement factor for the axial and helical tubes over a range of qualities for a mass flux of 225 kg/m^2-s (165 klb$_m$/ft^2-hr).

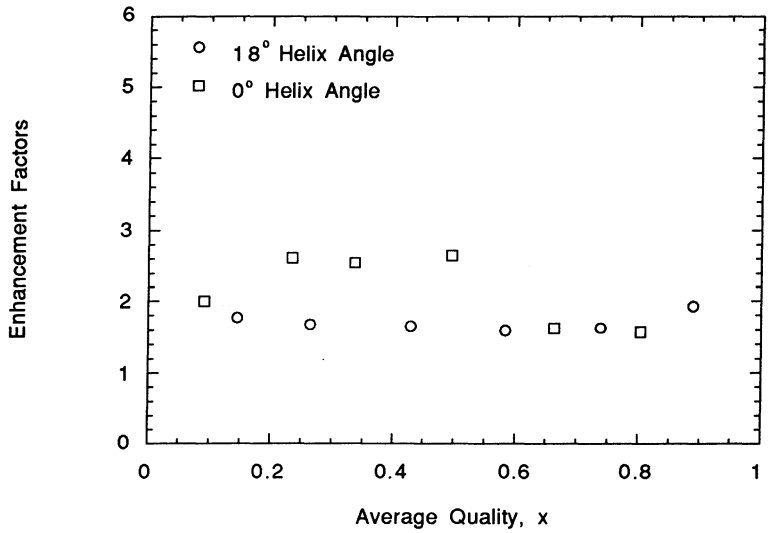

Figure 7 Enhancement factor for the axial and helical tubes over a range of qualities for a mass flux of 300 kg/m^2-s (220 klb$_m$/ft^2-hr).

Figs. 8 and 9 show a continued progression of the axial tube's region of high enhancement moving toward lower qualities as the mass flux continues to increase. The diminished enhancement effect relative to a smooth tube and the helical tube occurs at higher qualities. The drop in enhancement is generally occurring where the Froude number is 20 and the smooth tube flow is transitioning to an annular flow condition. Peak axial tube enhancement factors continue to show higher levels of enhancement. A mass flux of 400 kg/m^2-s (295 klb$_m$/ft^2-hr) shows peak enhancement factors of 2.7 while a mass flux of 450 kg/m^2-s (330 klb$_m$/ft^2-hr) reaches an enhancement level of 2.8. It is interesting to note that the helical tube continues to show an enhancement that generally reflects the area enhancement, rather than the pronounced enhancement effect shown by the axial tube. The helical tube seems to show a flow field configuration that consistently follows that of a smooth tube. That is, the relatively flat enhancement factor over the range of qualities where the smooth tube correlation switches from stratified wavy to annular flow configurations indicates that the helical tube transitions between these flow regions in a similar manner. It should also be noted that at higher mass fluxes and qualities, both axial and helical tubes show a trend toward enhancement levels that are less than their smooth tube area ratios.

Pressure drop characteristics of the axial tube, relative to the helical tube, are shown in Figs. 10 to 13 using the penalty factor defined by equation (10). Pressure drop data for mass fluxes below 225 kg/m^2-s (165 klb$_m$/ft^2-hr) are below the level of reliable resolution of the experiment's pressure transducer. Both tubes generally show that the micro-fin configuration results in low

penalty factors. The most interesting feature of these figures is the similarity in penalty factors for the axial and helical tubes. Even though the axial tube shows significant deviations from the helical tube's characteristics on a heat transfer basis, these effects do not show up in the pressure drop data.

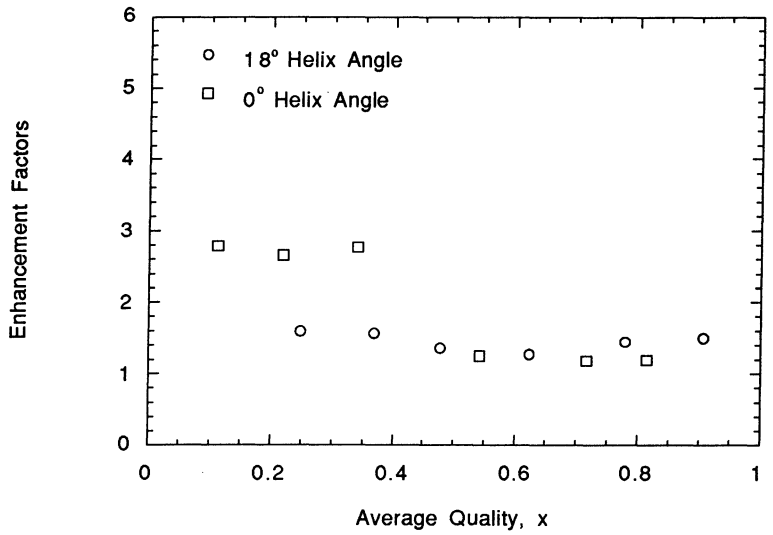

Figure 8 Enhancement factor for the axial and helical tubes over a range of qualities for a mass flux of 400 kg/m^2-s (295 klb$_m$/ft^2-hr).

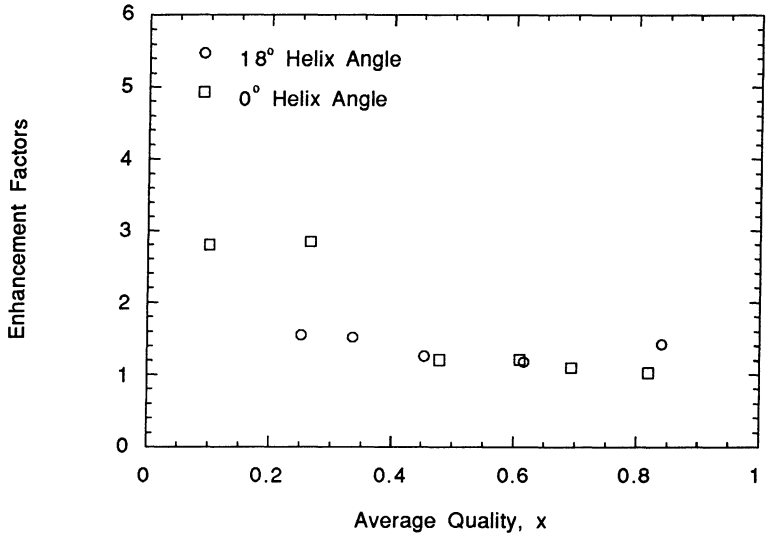

Figure 9 Enhancement factor for the axial and helical tubes over a range of qualities for a mass flux of 450 kg/m^2-s (330 klb$_m$/ft^2-hr).

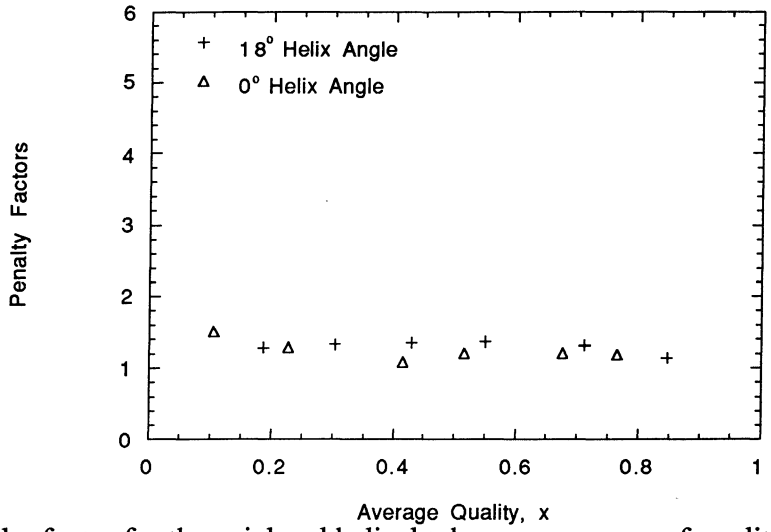

Figure 10 Penalty factor for the axial and helical tubes over a range of qualities for a mass flux of 225 kg/m^2-s (165 klb$_m$/ft^2-hr).

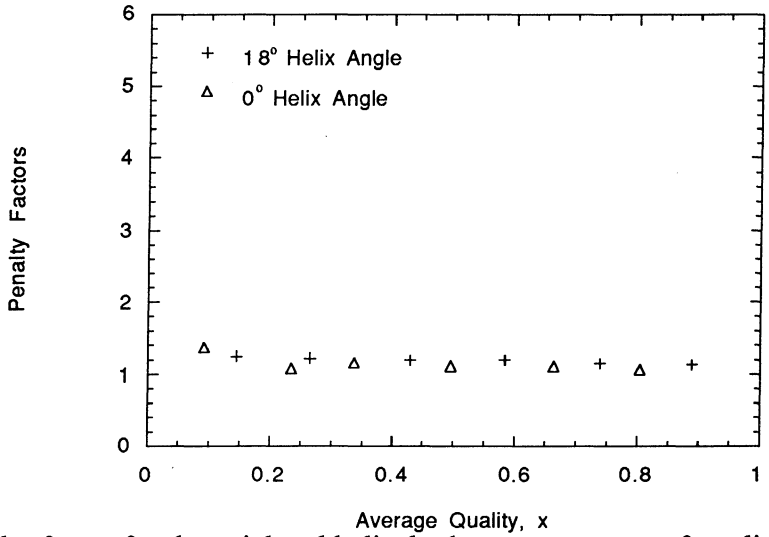

Figure 11 Penalty factor for the axial and helical tubes over a range of qualities for a mass flux of 300 kg/m^2-s (220 klb$_m$/ft^2-hr).

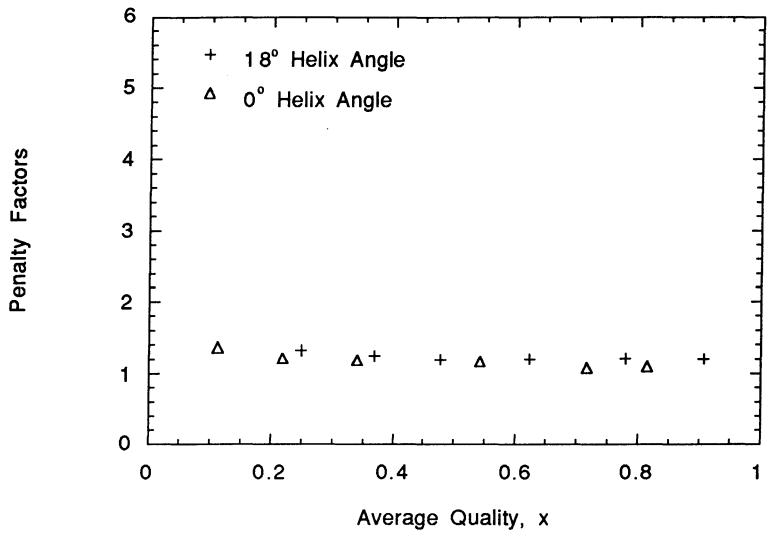

Figure 12 Penalty factor for the axial and helical tubes over a range of qualities for a mass flux of 400 kg/m^2-s (295 klb$_m$/ft^2-hr).

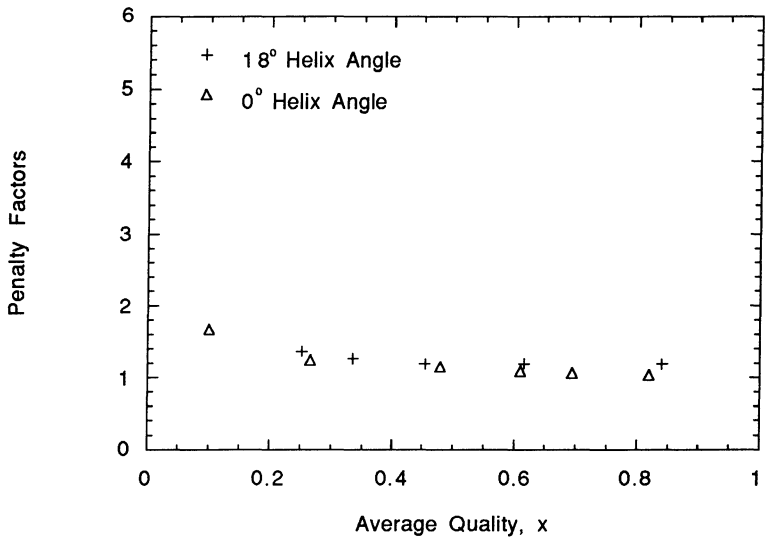

Figure 13 Penalty factor for the axial and helical tubes over a range of qualities for a mass flux of 450 kg/m^2-s (330 klb$_m$/ft^2-hr).

Hurlburt and Newell [19] have examined the transition between stratified flow and annular flow and have found that a "Froude rate" parameter indicates a transition between the two flow configurations. For the refrigerant conditions investigated in this study, numerical values for the Froude rate are similar to those for the Froude number. Over an extended range of conditions where variation of an annular flow's film thickness is of interest, the Froude rate parameter is significantly different and appropriately determines the characteristics of the flow field. The Froude rate parameter is defined as:

$$Ft = [m_v V_v^2/(m_l g D)]^{1/2} \tag{18}$$

The Froude rate, as seen above, is a ratio related to the vapor's power due to its kinetic energy to the power required to pump liquid from the bottom of the tube to the top of the tube. Alternatively, the Froude rate can be written in terms of refrigerant mass flux and quality.

$$Ft = [x^3 G^2/(\rho_v^2 g D(1-x))]^{1/2} \tag{19}$$

The transition between stratified flow and a non-uniform annular film flow is observed when one plots a "symmetry" parameter; the ratio of average film thickness to the bottom film thickness, versus the Froude rate. Unlike typical flow regime maps, this method for determining the transition between stratified and annular flow regions distinguishes between a "true" stratified flow and a non-uniform annular film flow. Local film thickness data is required in order to determine the transition point. For air-water systems, the Froude rate shows the transition region in smooth tubes to be near a value of 20. No local film thickness measurement data has been found for refrigerant-type substances. However, assuming similar trends occur, one would expect that a similar level of energy is required from the vapor for distributing liquid around the periphery of the tube.

Fig. 14 shows axial tube enhancement factors plotted versus the Froude rate parameter for all the experimental data. The plot shows that the region of high enhancement, relative to smooth tubes and the helical tube, occurs between Froude rate values of 1 and 20. A closer examination of the trends is shown in Fig. 15 for axial tube data with Froude rates less than 20. The different character of the 75 kg/m^2-s (55 klb$_m$/ft^2-hr) mass flux relative to the higher mass fluxes is clearly seen in both Figs. 14 and 15. Fig. 14 shows that at Froude rates greater than 20, the relative enhancement is diminished with mass flux. Fig. 15 shows that peak enhancement levels obtained in the high enhancement region increase with mass flux. Also shown in Fig. 15 is the sharp drop in enhancement as Froude rates decrease below 1 to 2. Based on Figs. 14 and 15, the axially grooved tube appears to maintain an annular flow configuration that is more efficient than the

stratified flow configuration found in smooth tubes. The helical tube appears to maintain a flow configuration similar to that of a smooth tube.

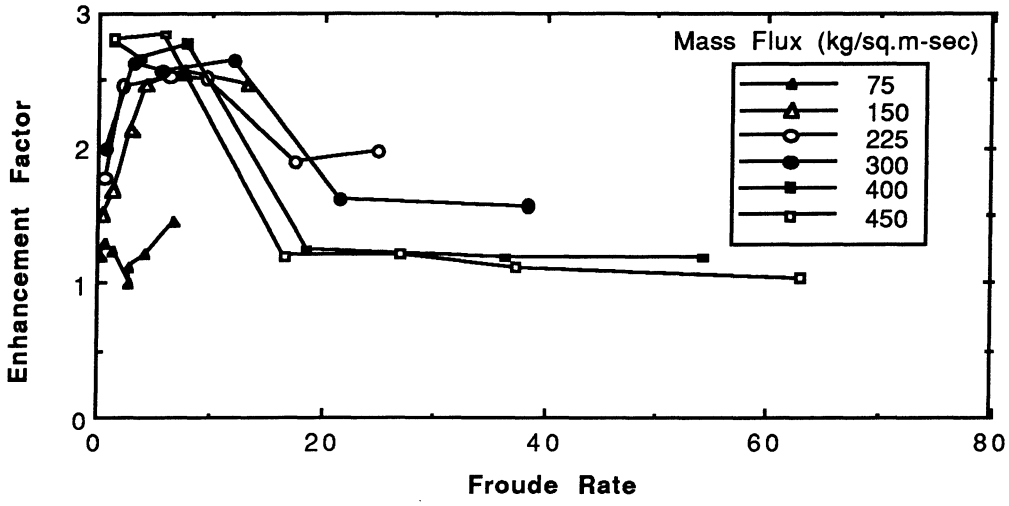

Figure 14 Plot of axial tube enhancement factors versus the Froude rate parameter for all axial tube data.

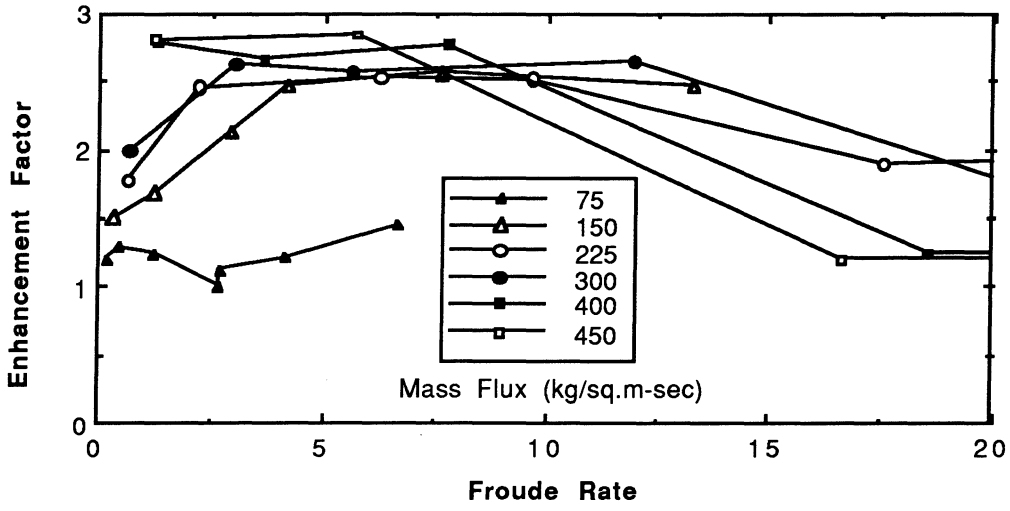

Figure 15 Plot of the axial tube enhancement factors versus the Froude rate parameter for Froude rate data less than 20.

Fig. 16 is a parametric plot of Froude rate versus mass flux for R134a at 35 °C (95°F) in an 8 mm (.315") inside diameter tube. Lines of constant quality from 0.1 to 0.8 are also marked on Fig. 16. A region between Froude rates of 1 and 20 and mass fluxes from 150 to 450 kg/m^2-s (110 to 330 klb$_m$/ft^2-hr) is outlined in order to show the range where an axial tube would have enhancements significantly above those of a helical tube. At the low mass flux range, qualities from 0.2 to 0.8 would be significantly enhanced. Mid-range to higher range mass fluxes of 300 to 450 kg/m^2-s (220 to 330 klb$_m$/ft^2-hr) would enhance heat transfer between qualities of 0.1 and 0.6.

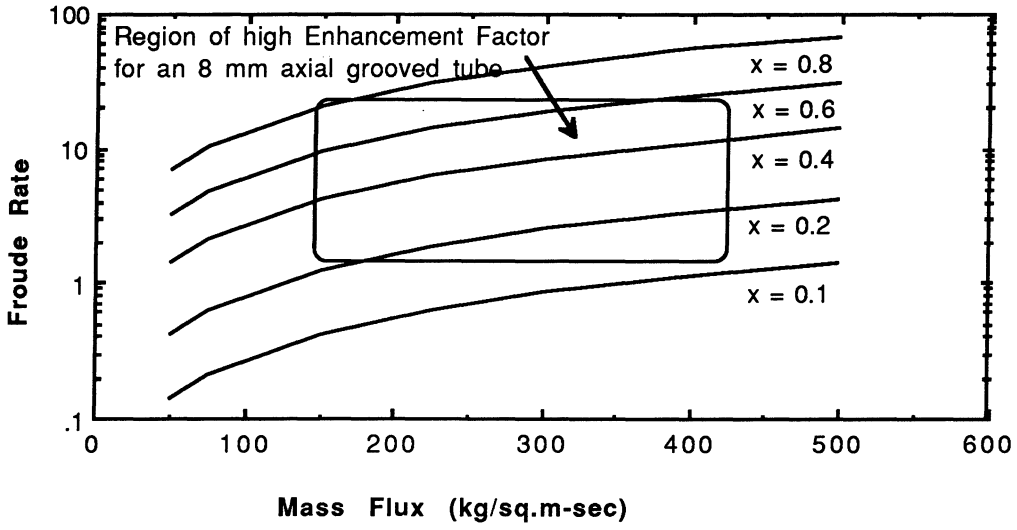

Figure 16 Plot showing an estimated region for an 8 mm diameter tube in which axial grooves may result in significant performance over helical and smooth tubes.

It should be noted that an alternative approach to be considered in the data reduction is to not use the equivalent flow diameter when calculating the Froude rate. Instead, if one recognizes that the denominator in the Froude rate is the power required to pump liquid from the bottom of the tube to the top of the tube, it might be more accurate when looking at an axial micro-finned tube to consider the power required to pump the liquid from one fin to the next. For example, the tube considered in this study had sixty trapezoidal fins. Therefore, in order to get from the bottom of the tube to the top, the liquid must go over 20 to 30 fins. If one considers only the power required to go from one fin to the next, the total Froude rate would increase by a factor of twenty to thirty.

CONCLUSIONS

Axial micro-fin grooving shows a region of significant heat transfer enhancement when compared to a similarly grooved helical tube. Results show the enhanced heat transfer to be dependent on the mass flux and quality of the refrigerant. A Froude rate parameter provides a basis for correlating the region of enhancement over the mass flux and quality ranges studied. The level of enhancement also appears to be dependent on mass flux. Higher mass fluxes have higher levels of peak enhancement. In terms of pressure drop, the axial tube has a penalty factor that is equivalent to the helical tube.

Future questions to be answered relate to the extension of these results to other conditions. Higher pressure refrigerants (such as R22 with higher vapor densities) and lower pressure refrigerants (such as R123 with lower vapor densities) should be examined. Geometric dependencies should also be examined. The effects of groove geometry and tube diameter variations are unknown. Finally, the effect of oil and its ability to "clog" grooves should be examined.

ACKNOWLEDGMENTS

The authors appreciate the financial support of the UIUC Air Conditioning and Refrigeration Center, an NSF sponsored, Industry supported research center. Modine Manufacturing Company is thanked for special fabrication of axially grooved tubes with dimensions matching their 18 degree helix tube.

REFERENCES

1 Chiang, R., 1993, "Heat Transfer and Pressure Drop During Evaporation and Condensation of Refrigerant-22 in 7.5 mm and 10 mm Diameter axial and Helical Grooved Tubes", AIChE Heat Transfer Symposium, Atlanta, No. 295, Vol. 89, pp. 205- 210.

2 Dobson, M. K., 1994, "Heat Transfer and Flow Regimes During Condensation in Horizontal Tubes," Ph.D. thesis, University of Illinois at Urbana-Champaign.

3 Eckels, S.J. and Pate, M.B., 1991, "Evaporation and Condensation of HFC-134a and CFC-12 in a Smooth and a Micro-fin Tube", ASHRAE Transactions, No. 2, Vol. 97, pp. 71-81.

4 Luu, M. and A.E. Bergles, 1979, "Experimental Study of the Augmentation of In-Tube Condensation of R-113", ASHRAE Transactions, No. 3, Vol. 85, 132-145.

5 Ponchner, M. and J. C. Chato, 1995, "Condensation of HFC-134a in an 18° Helix Angle Micro-Finned Tube," ACRC Report TR-75, University of Illinois at Urbana-Champaign.

6 Ponchner, M., 1995, "Condensation of HFC-134a in an 18° Helix Angle Micro-Finned Tube," M.S. Thesis, University of Illinois at Urbana-Champaign.

7 Khanpara, J.C., 1986, "Augmentation of In-Tube Evaporation and Condensation with Micro-fin Tubes using Refrigerants R-113 and R-22", Ph.D. thesis, Iowa State University.

8 Schlager, L.M., M.B. Pate and A.E. Bergles, 1988a, "Evaporation and Condensation of Refrigerant-Oil Mixtures in a Smooth Tube and Micro-Fin Tube", ASHRAE Trans. 94, part 1, 149-166.

9 Schlager, L.M., M.B. Pate and A.E. Bergles, 1988b, "Evaporation and Condensation of Refrigerant-Oil Mixtures in a Low-Fin Tube", ASHRAE Trans. 94 part 2, 1176-1194.

10 Schlager, L.M., M.B. Pate and A.E. Bergles, 1989, "A Comparison of 150 and 300 SUS Oil Effects on Refrigerant Evaporation and Condensation in a Smooth Tube and a Micro-Fin Tube", ASHRAE Trans. 95 part 1, 387-397.

11 Schlager, L.M., M.B. Pate and A.E. Bergles, 1990a, "Performance Predictions of Refrigerant-Oil Mixtures in Smooth and Internally Finned Tubes-Part I: Literature Review", ASHRAE Trans. 96 part 1, 160-171.

12 Schlager, L.M., M.B. Pate and A.E. Bergles, 1990b, "Performance Predictions of Refrigerant-Oil Mixtures in Smooth and Internally Finned Tubes- Part II: Design Equations", ASHRAE Trans. 96 part 1, 170-182.

13 Sur, B. and N.Z. Azer, 1991, "Effect of Oil on Heat Transfer and Pressure Drop During Condensation of Refrigerant-113 Inside Smooth and Internally Finned Tubes", ASHRAE Trans., 365-373.

14 Lockhart, R.W., and R.C. Martinelli, 1947, "Proposed Correlation of Data For Isothermal Two-Phase, Two-Component Flow in Pipes", Chemical Engineering Progress, 45(1), 39-48.

15 Soliman, H.M., 1982, "On the Annular-To-Wavy Flow Pattern Transition During Condensation Inside Horizontal Tubes", The Canadian Journal of Chemical Engineering, 60, 475-481.

16 Souza, A.M., J.C. Chato, J.P. Wattelet, and B.R. Christoffersen, 1993, "Pressure Drop During Two-Phase Flow of Pure Refrigerants and Refrigerant-Oil Mixtures in Horizontal Smooth Tubes", ASME, HTD-Vol. 243, 35-41.

17 Souza, A.M., J.C. Chato, and J.P. Wattelet, 1992, "Pressure Drop During Two-Phase Flow of Refrigerants in Horizontal Smooth Tubes", ACRC Report TR-25, University of Illinois at Urbana-Champaign.

18 Zivi, S.M., 1964, "Estimation of the Steady-State Void-Fraction by Means of the Principle of Minimum Entropy Production", Journal of Heat Transfer, 86, 247-252.

19 Hurlburt, E.T. and Newell, T.A., 1997, "Prediction of the Circumferential Film Thickness Distribution in Horizontal Annular Gas-Liquid Flow", submitted to Int. J. Multiphase Flow.